

Supporting Information for:

Between Descriptors and Properties: Understanding the Ligand Efficiency Trends for GPCR and Kinase Structure Activity Data Sets

Jaroslaw Polanski^a*, Aleksandra Tkocz^a

^a*Institute of Chemistry, University of Silesia, 9 Szkolna Street, 40-006 Katowice, Poland*

Corresponding Author

[*polanski@us.edu.pl](mailto:polanski@us.edu.pl)

TABLE OF CONTENTS

FIGURE S1. Distribution of $\log K_i$ (**a-c**) and $\log IC_{50}$ (**d-f**) for GPCR1, GPCR2 and kinase data.

FIGURE S2. Distribution of MW for K_i (**a-c**) and IC_{50} (**d-f**) subdata.

FIGURE S3. Distribution of HAC for K_i (**a-c**) and IC_{50} (**d-f**) subdata.

FIGURE S4. Variable distribution for 5HT2A subdata: **a)** $\log K_i$ (GPCR 1) , **b)** MW (GPCR 1), **c)** HAC (GPCR 1), **d)** $\log K_i$ (GPCR 2), **e)** MW (GPCR 2), **f)** HAC (GPCR 2), **g)** $\log IC_{50}$ (GPCR 1), **h)** MW (GPCR 1), **i)** HAC (GPCR 1), **j)** $\log IC_{50}$ (GPCR 2), **k)** MW (GPCR 2), **l)** HAC (GPCR 2).

FIGURE S5. Variable distribution for 5HT2B K_i (**a-f**) and IC_{50} (**g-l**) subdata **a)** $\log K_i$ (GPCR 1), **b)** MW (GPCR 1), **c)** HAC (GPCR 1), **d)** $\log K_i$ (GPCR 2), **e)** MW (GPCR 2), **f)** HAC (GPCR 2), **g)** $\log IC_{50}$ (GPCR 1), **h)** MW (GPCR 1), **i)** HAC (GPCR 1), **j)** $\log IC_{50}$ (GPCR 2) , **k)** MW (GPCR 2), **l)** HAC (GPCR 2).

FIGURE S6. Variable distribution for Abl1 K_i (**a-c**) and IC_{50} (**d-f**) subdata **a)** $\log K_i$, **b)** MW, **c)** HAC, **d)** $\log IC_{50}$, **e)** MW, **f)** HAC.

FIGURE S7. Variable distribution for CDK2 K_i (**a-c**) and IC_{50} (**d-f**) subdata **a)** $\log K_i$, **b)** MW, **c)** HAC, **d)** $\log IC_{50}$, **e)** MW, **f)** HAC.

FIGURE S8. A comparison of BEI vs. MW and LE vs. HAC plots for kinase- Abl1 and GPCR- 5HT2A data; **a-c)** BEI ($\log K_i/MW$) vs. MW; **d-f)** BEI ($\log IC_{50}/MW$) vs. MW; **g-i)** LE ($\log K_i/HAC$) vs. HAC; **j-l)** LE ($\log IC_{50}/HAC$) vs. HAC.

FIGURE S9. A comparison of BEI vs. MW and LE vs. HAC for kinase- CDK2 and GPCR- 5HT2B data; **a-c)** BEI ($\log K_i/MW$) vs. MW; **d-f)** BEI ($\log IC_{50}/MW$) vs. MW; **g-i)** LE ($\log K_i/HAC$) vs. HAC; **j-l)** LE ($\log IC_{50}/HAC$) vs. HAC.

FIGURE S10. A relationship of $BEI = \log K_i/MW$ vs. $1/MW$, correlation coefficient: $R= 0,60; 0,58;$ $0,65$ for **(a-c)**, respectively, and $BEI = \log IC_{50}/MW$ vs. $1/MW$, correlation coefficient: $R= 0,73; 0,69;$ $0,68$ for **(d-f)**, respectively.

FIGURE S11. A relationship of $LE = \log K_i/HAC$ vs. $1/HAC$, **(a-c)**, and $\log IC_{50}/HAC$ vs. $1/HAC$, **(d-f)** respectively.

FIGURE S1. Distribution of $\log K_i$ (a-c) and $\log IC_{50}$ (d-f) for GPCR1, GPCR2 and kinase data.

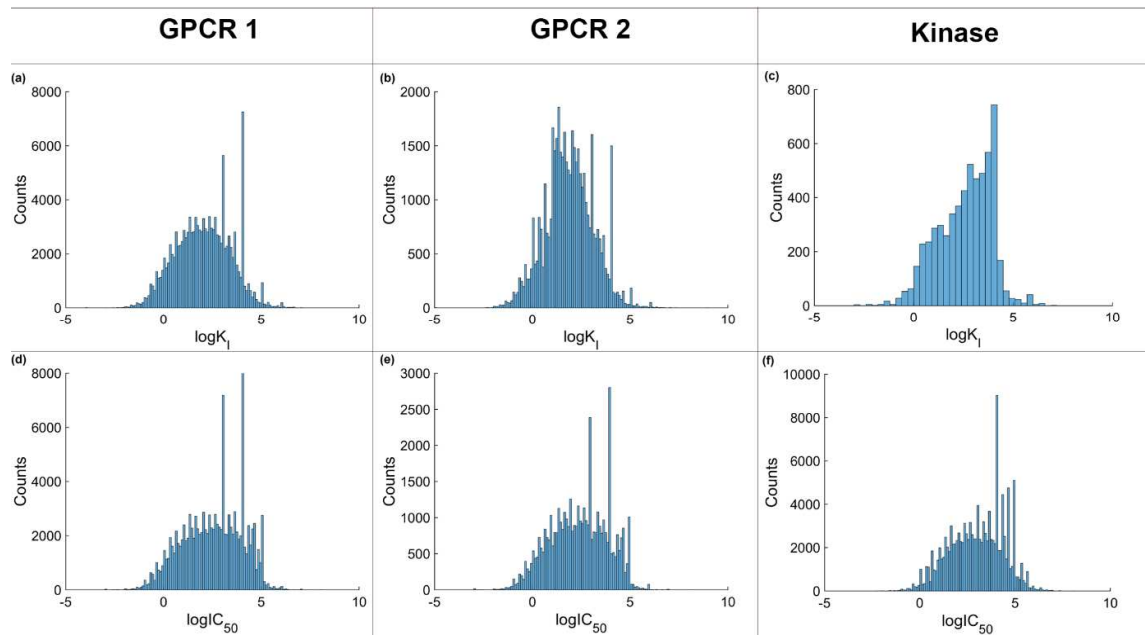


FIGURE S2. Distribution of MW for K_i (**a-c**) and IC_{50} (**d-f**) subdata.

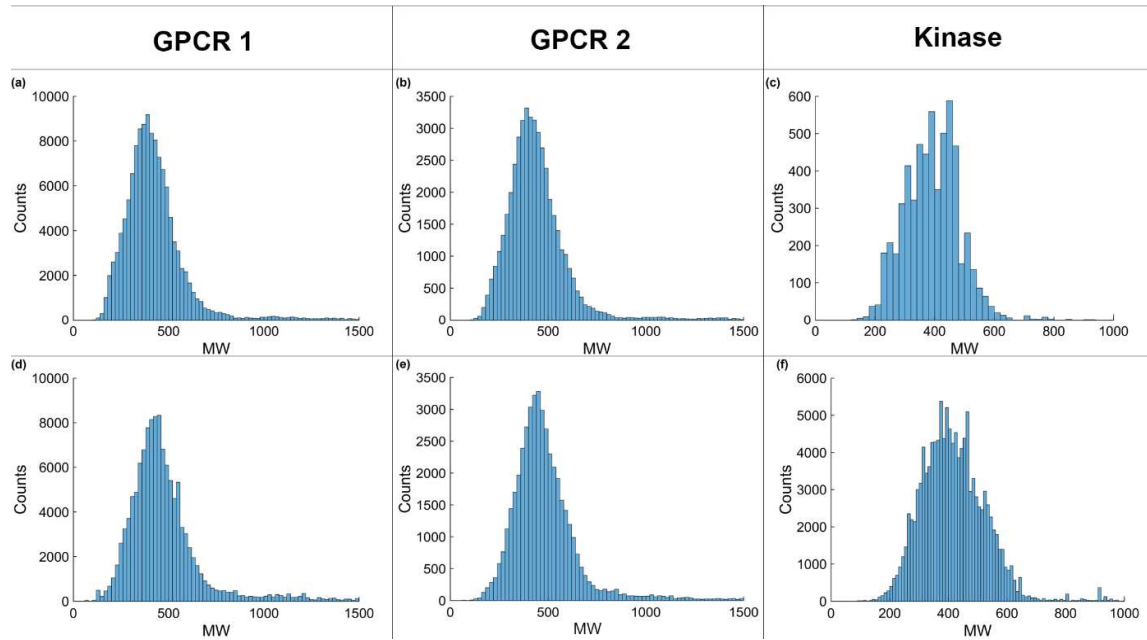


FIGURE S3. Distribution of HAC for K_i (**a-c**) and IC_{50} (**d-f**) subdata.

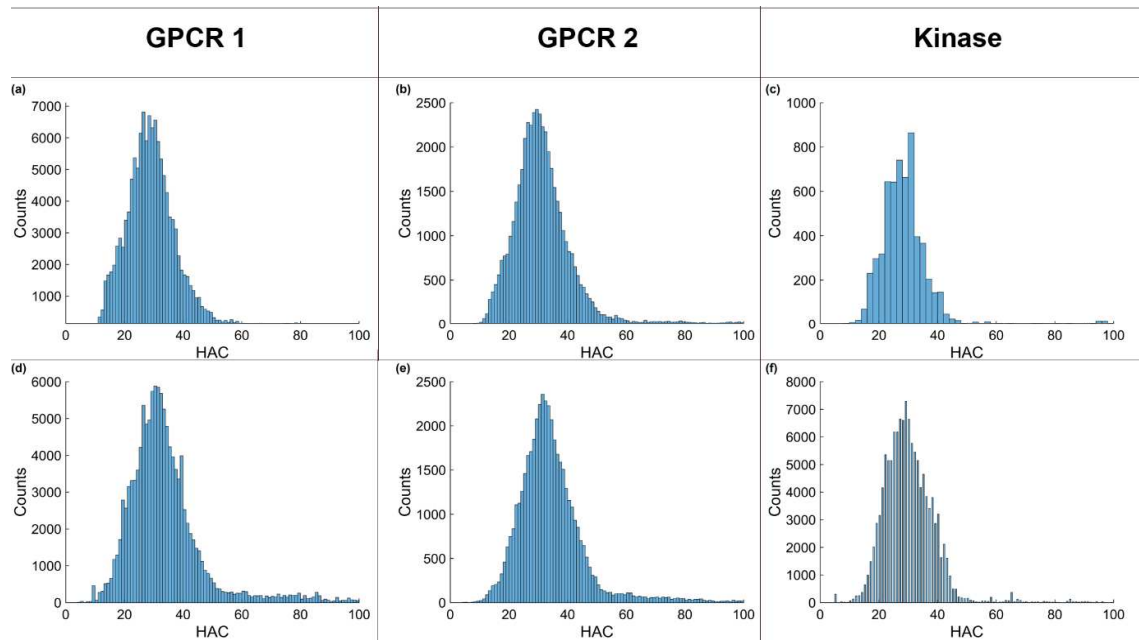


FIGURE S4. Variable distribution for 5HT2A subdata: **a)** logK_i (GPCR 1) , **b)** MW (GPCR 1), **c)** HAC (GPCR 1), **d)** logK_i (GPCR 2), **e)** MW (GPCR 2), **f)** HAC (GPCR 2), **g)** logIC₅₀ (GPCR 1), **h)** MW (GPCR 1), **i)** HAC (GPCR 1), **j)** logIC₅₀ (GPCR 2), **k)** MW (GPCR 2), **l)** HAC (GPCR 2).

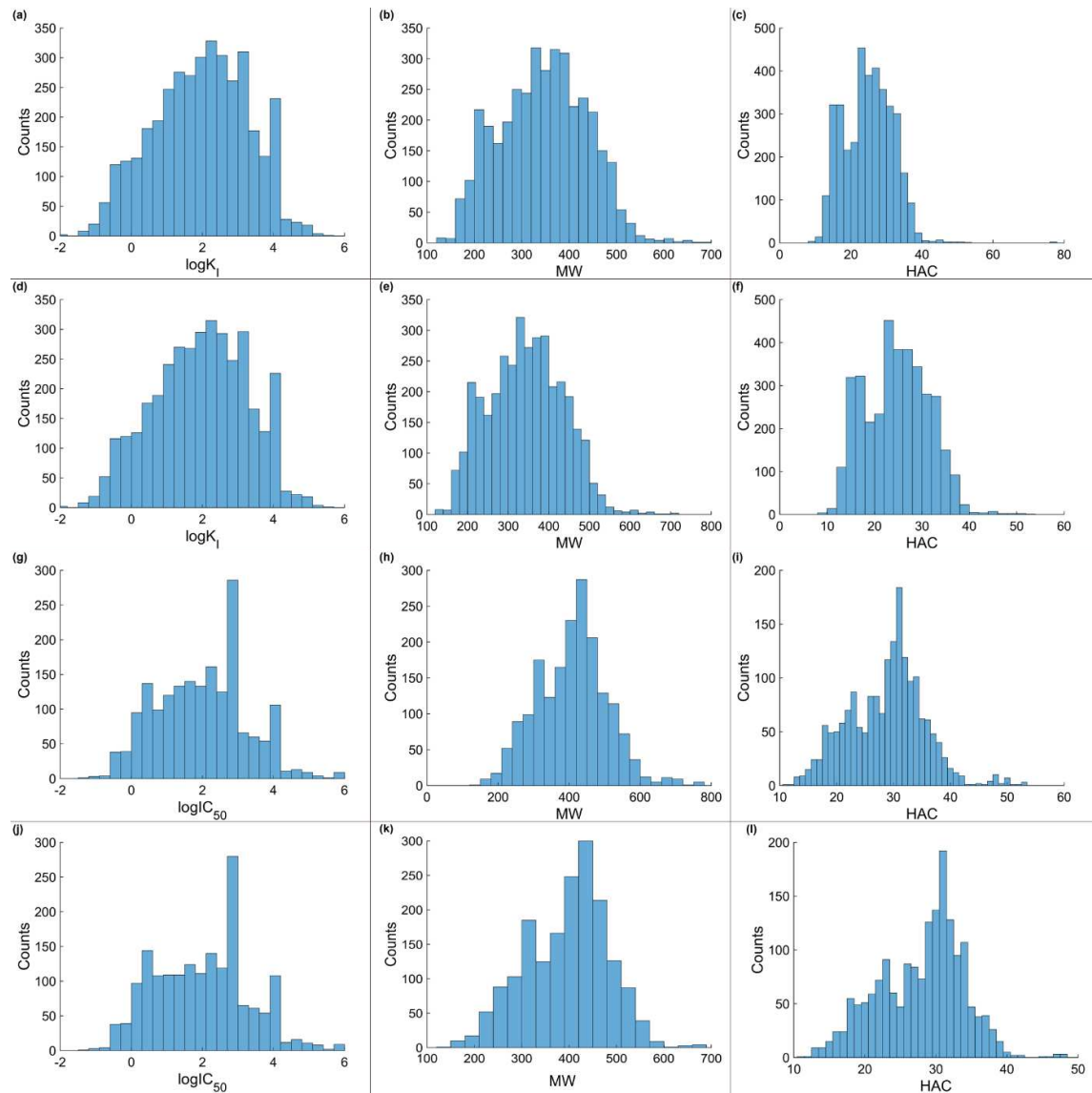


FIGURE S5. Variable distribution for 5HT2B K_i (a-f) and IC₅₀ (g-l) subdata **a)** logK_i (GPCR 1), **b)** MW (GPCR 1), **c)** HAC (GPCR 1), **d)** logK_i (GPCR 2), **e)** MW (GPCR 2), **f)** HAC (GPCR 2), **g)** logIC₅₀ (GPCR 1), **h)** MW (GPCR 1), **i)** HAC (GPCR 1), **j)** logIC₅₀ (GPCR 2), **k)** MW (GPCR 2), **l)** HAC (GPCR 2).

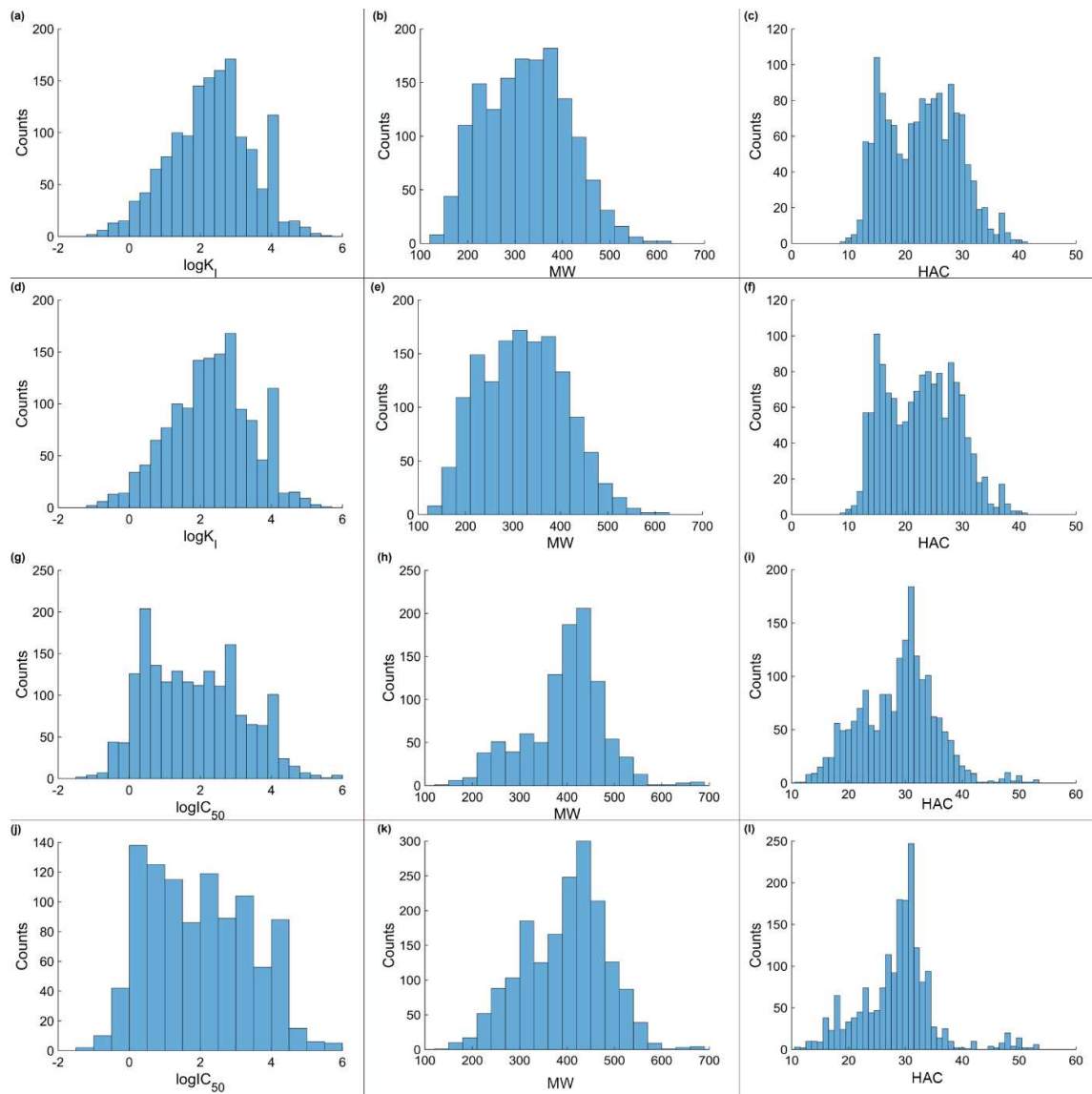


FIGURE S6. Variable distribution for Abl1 K_i (a-c) and IC₅₀ (d-f) subdata **a)** logK_i, **b)** MW, **c)** HAC, **d)** logIC₅₀, **e)** MW, **f)** HAC.

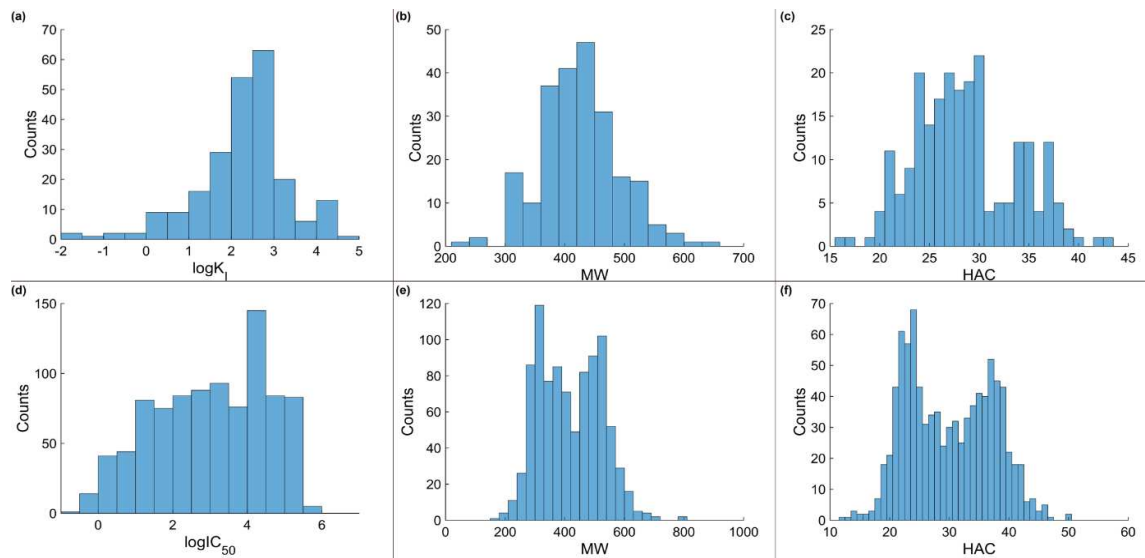


FIGURE S7. Variable distribution for CDK2 K_i (a-c) and IC₅₀ (d-f) subdata **a)** logK_i, **b)** MW, **c)** HAC, **d)** logIC₅₀, **e)** MW, **f)** HAC.

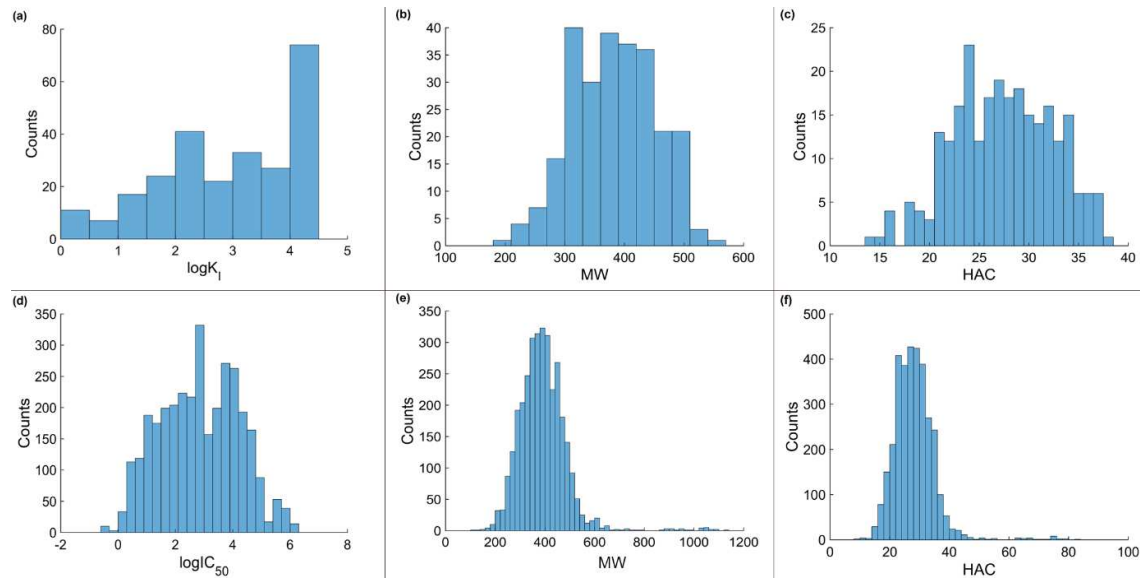


FIGURE S8. A comparison of BEI vs. MW and LE vs. HAC plots for kinase- Ab11 and GPCR- 5HT2A data; **a-c**) BEI ($\log K_i/MW$) vs. MW; **d-f**) BEI ($\log IC_{50}/MW$) vs. MW; **g-i**) LE ($\log K_i/HAC$) vs. HAC; **j-l**) LE ($\log IC_{50}/HAC$) vs. HAC.

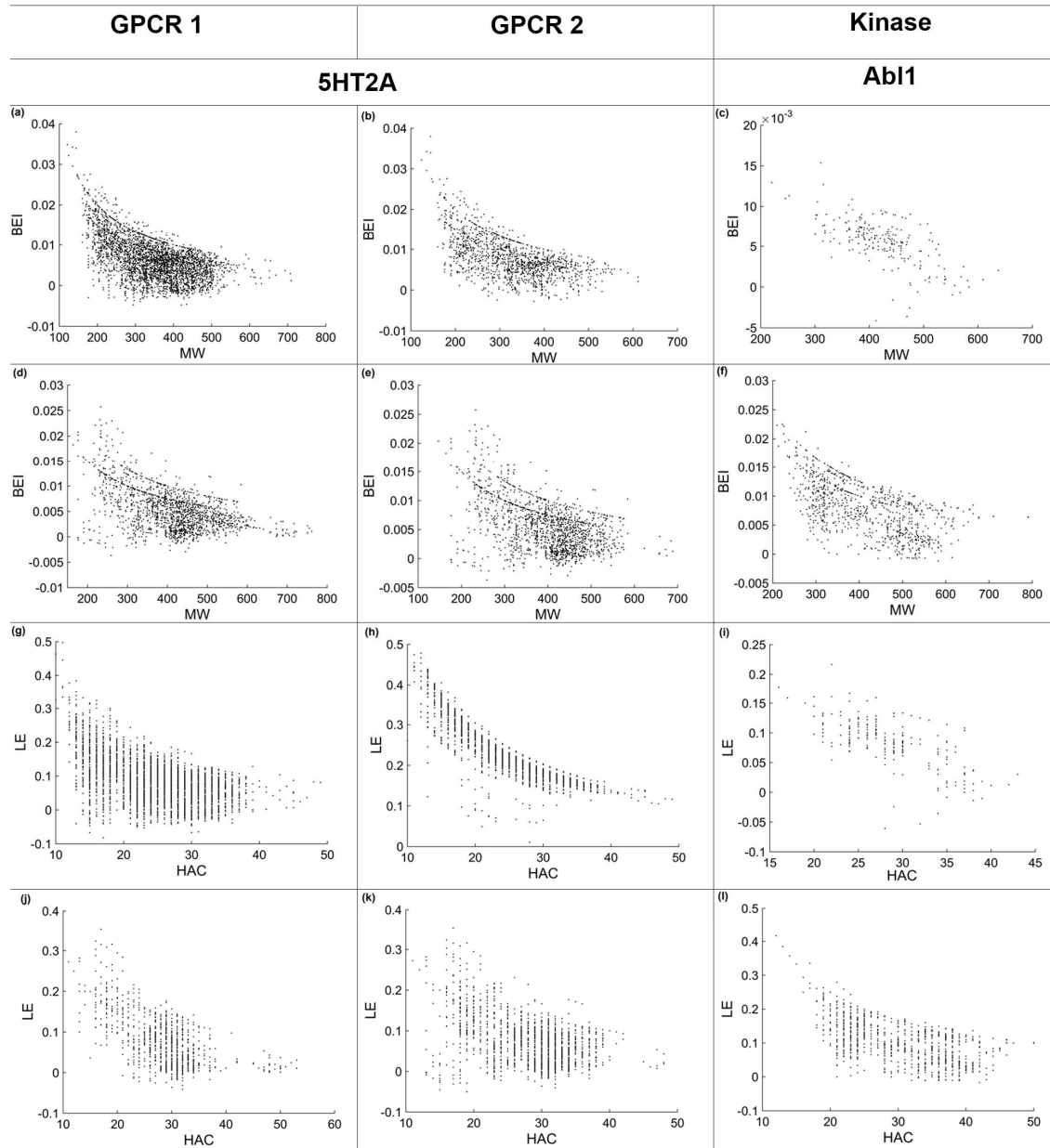


FIGURE S9. A comparison of BEI vs. MW and LE vs. HAC for kinase- CDK2 and GPCR- 5HT2B data; **a-c)** BEI ($\log K_i/MW$) vs. MW; **d-f)** BEI ($\log IC_{50}/MW$) vs. MW; **g-i)** LE ($\log K_i/HAC$) vs. HAC; **j-l)** LE ($\log IC_{50}/HAC$) vs. HAC.

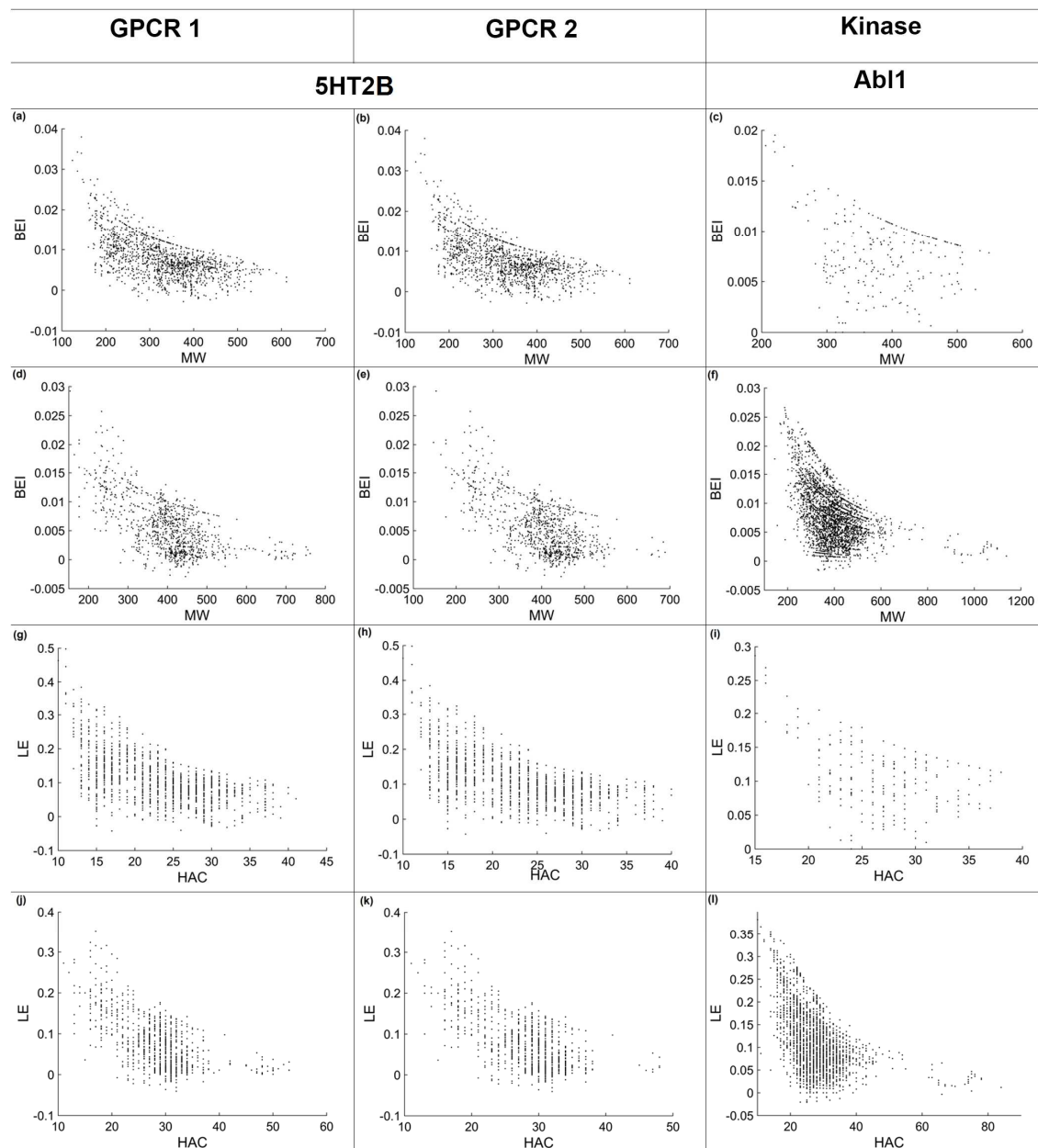


FIGURE S10. A relationship of BEI= $\log K_i/MW$ vs. $1/MW$, correlation coefficient: R= 0,60; 0,58; 0,65 for (a-c), respectively, and BEI= $\log IC_{50}/MW$ vs. $1/MW$, correlation coefficient: R= 0,73; 0,69; 0,68 for (d-f), respectively.

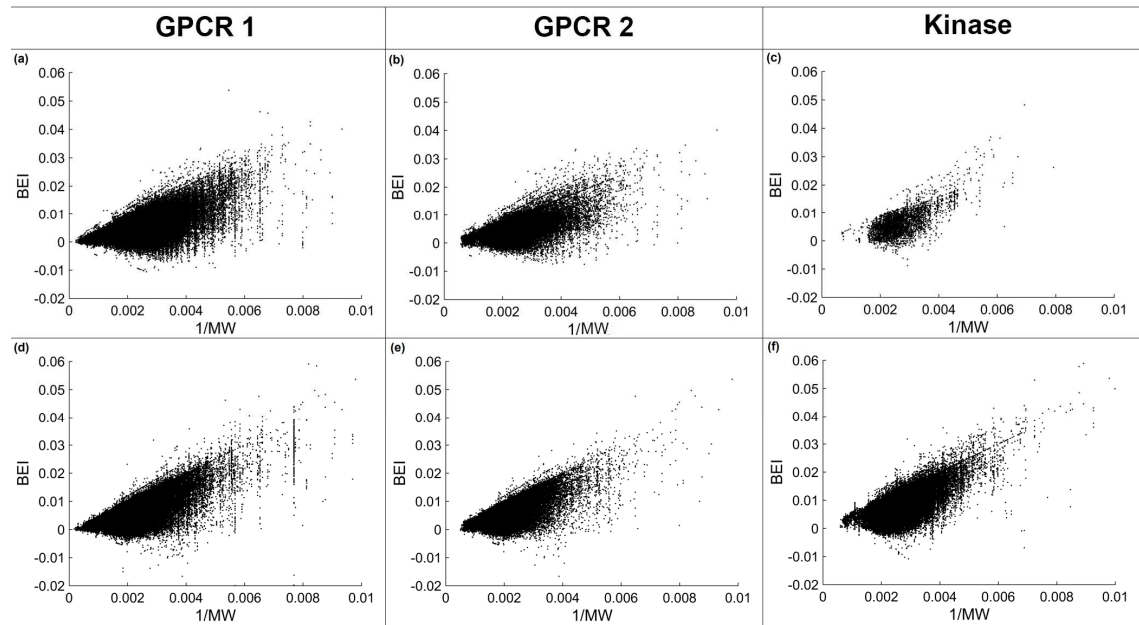


FIGURE S11. A relationship of LE= $\log K_i/\text{HAC}$ vs. $1/\text{HAC}$, **(a-c)**, and $\log IC_{50}/\text{HAC}$ vs. $1/\text{HAC}$, **(d-f)**, respectively.

